Analysis of Cytoskeleton-Destabilizing Agents by Optimized Optical Navigation and AFM Force Measurements

A. Berquand[1] *, A. Holloschi[2], M. Trendelenburg[2], and P. Kioschis[2]
[1]Veeco Instruments GmbH, Dynamostrasse 19, Mannheim, Germany 68165
[2]University of Applied Sciences, Institute of Molecular and Cell Biology, Windeckstr. 110, Mannheim, Germany 68163
* aberquand@veeco.de

Introduction

Mechanical properties of cells are determined by the dynamic behavior of the cytoskeleton and physical interactions with the environment. The cytoskeleton, composed of actin filaments, intermediate filaments, and microtubules, is vital for numerous key cellular processes, such as cell division, vesicle trafficking, cell contraction, cell motility, and cell signaling. There is increasing evidence that deregulation of cytoskeletal components like disassembly of actin and tubulin filaments is an important parameter in cellular pathology. Thus, significant alterations of the mechanical phenotype of the cell and its surrounding microenvironment are reported to be involved in aberrant cellular processes and successively contribute to onset and progression of diseases such as cancer, malaria, and possibly neurodegeneration [1–5]. *In vitro* and ex vivo biomechanical studies have shown that cancer cells have significantly decreased elastic moduli than their normal counterparts, a characteristic that is attributed to the ability of cancer cells to metastasize or spread [6, 7].

Along with other techniques, atomic force microscopy (AFM) has become a powerful method to explore mechanical properties of living cells in nearly physiological conditions [8,9] and even of ex vivo cancer cells [6]. Living cells typically show a Young's modulus between 0.5 and 200 kPa depending on sub-cellular region and cell type. These specific mechano-biological properties can be quantified by AFM force measurements and subsequently used to assess and correlate effects of drug treatment, aging, or pathology [10–14].

In this article, we used Multiple Image Registration Overlay (MIRO) software and the Bioscope Catalyst Atomic Force Microscope (Veeco Instruments, Santa Barbara, CA) to facilitate optical navigation targeting the best locations for force measurements in living cells. This approach was used to explore real-time changes in cell integrity of two cancer cell lines, HeLa and U2-O2 osteosarcoma, upon treatment with the cytoskeleton-destabilizing drugs, nocodazole and latrunculin B. The apparent Young's moduli of these cells were quantified and compared. This allowed us to differentiate the visco-elastic changes caused by the disassembly of the actin cytoskeleton from those caused by the disassembly of the microtubule network. Furthermore, it enabled us to discriminate the two types of cancer cells based on their elastic properties.

Experimental Setup

Cell lines and sample preparation. Experiments were carried out on HeLa cells as well as on two recombinant osteosarcoma cell lines, U2-OS-FP635-Actin and U2-OS-Tag-RFP-Tubulin, respectively (Marinpharm GmbH, Luckenwalde, Germany). The U2-OS-FP635-Actin cell line was generated by stable transfection of human osteosarcoma cells with far-red fluorescent protein FP635-tagged human beta-actin (Ex./Em. = 590/635 nm). The U2-OS-Tag-RFP-Tubulin cell line stably expresses Tag-RFP tagged β-tubulin (human) on human osteosarcoma cell background (Ex./Em. = 557/585 nm). Optimization of optical navigation utilizing MIRO software was performed on fixed HeLa cells. HeLa cells were grown on glass-bottom petri dishes (Willco) and stained for actin with Phalloidin-Alexa488 (Ex./Em. = 494/519 nm) (Invitrogen), and for tubulin with an anti-β-tubulin antibody (Ex./Em. = 550/570 nm) (Sigma) detected by a TRITC-labeled secondary antibody (Ex./Em. = 494/518 nm). In addition, the specimen was stained with DAPI targeting DNA in the cell nucleus (Ex./Em. = 358/461 nm).

In order to monitor drug response, living cells expressing fluorescently tagged fusions protein of actin and tubulin, respectively, were used. HeLa cells were transiently transfected with pEYFP-Actin or pEYFP-Tubulin plasmid (Clontech), or transiently co-transfected with pEYFP-Actin and pECFP-Tubulin. In the same way U2-OS-Tag-RFP Tubulin and U2-OS-Tag-FP635 Actin cells were either transfected with pEYFP-Actin or pEYFP-Tubulin. The transfected cells were grown on glass-bottom petri dishes and stained with DAPI (50 µM, 30 minutes at 37°C). In order to analyze distinct effects of drugs interfering with cytoskeletal integrity, cells were treated with cytoskeleton destabilizing agents latrunculin (disruption of the actin cytoskeleton) and nocodazole (disruption of microtubules), respectively. Treatment of cells with nocodazole or latrunculin was performed at a concentration of 50 µM for 30 minutes at room temperature. Drugs were applied directly to the cells in the glass-bottom petri dishes. Thus, the permeabilization step, which can rapidly lead to cell death, was omitted. Finally, the samples were rinsed twice and imaged in 1× phosphate buffered saline (PBS). All experiments were performed at room temperature 24 hours after transfection.

AFM measurements and data processing. Imaging and force measurements were performed with two separate BioScope™ Catalyst™ Atomic Force Microscope systems that were fully integrated with inverted optical microscopes. One system used a Leica DMI 6000 with a Hamamatsu ORCA camera, and the other used a Zeiss Axio Observer with an AxioCam camera. Several AFM probes (Veeco MLCT, SNL, MSNL) were utilized during the experiments; however, the same tip was used before and after drug delivery to avoid the influence of tip shape and spring constant when comparing the force curves. Force measurements were done by using

Put the Knowledge and Experience of an EDS Expert to Work for You

...and Change the Way You do Analysis Forever

B Kα, Si Kα...5 kV...ZAF > X?

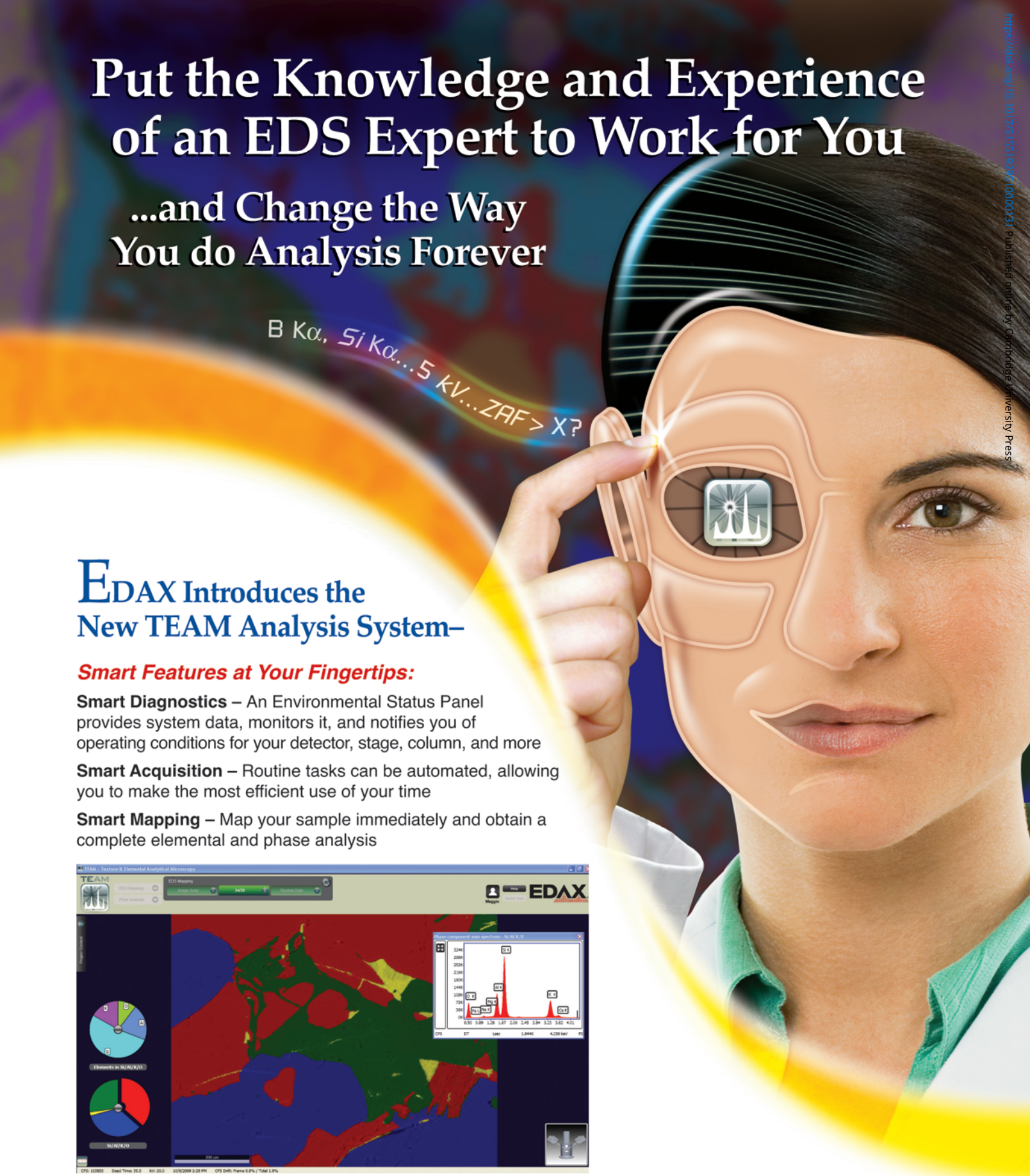

EDAX Introduces the New TEAM Analysis System–

Smart Features at Your Fingertips:

Smart Diagnostics – An Environmental Status Panel provides system data, monitors it, and notifies you of operating conditions for your detector, stage, column, and more

Smart Acquisition – Routine tasks can be automated, allowing you to make the most efficient use of your time

Smart Mapping – Map your sample immediately and obtain a complete elemental and phase analysis

TEAM Up with EDAX for SMART EDS Analysis.
Visit our website at ***www.EDAX.com/TEAMSMART***
or call ***1-201-529-4880****.*

AMETEK®
MATERIALS ANALYSIS DIVISION

Visit Us at the MRS Spring Meeting

EDAX®
advanced microanalysis solutions

MLCT-C cantilevers having nominal spring constant of 0.01 N/m calibrated on a stiff part of the dish (glass). Deflection sensitivities were found to be between 23.57 and 76.83 nm/V. Force volume images were achieved by using the following parameters: scan size of 2 µm, scan rate of 3 Hz, surface delay of 10 ms, retract delay of 100 ms and trigger threshold of 50 nm. The same cantilevers were used for contact mode imaging, but MLCT-E and -F (nominal spring constants of 0.1 and 0.5 N/m, respectively) were used for tapping mode imaging.

Veeco's Microscope Image Registration and Overlay (MIRO) software provided a simple and quick way to navigate the tip to an area of choice to perform the AFM measurements. The registration can be done using either three points or fourth- or fifth-order polynomial calibration (for non-ideal light microscopy conditions). Cross-sections made from the topographical images have shown that the average height of selected cell areas for force measurements (Figure 1) was at least 170 nm. In Force Volume mode, the tip is basically sensitive to the first tenth of nanometers. Therefore, influences of the glass substrate on the recorded indentation curves are unlikely.

Results

Though the primary advantage of Veeco Multiple Image Registration Overlay (MIRO) software is based on automatically overlaying light optical and AFM images, in these studies we also utilized MIRO to target best locations for force measurements. Optimization of this procedure was performed using fixed HeLa cells as well as living U2-OS-Tag-RFP Tubulin cells transfected with pEYFP-Actin. Figure 1 shows a real-time overlay of the fluorescence emission signal of actin and tubulin networks with the correlating high-resolution AFM topography image of membrane surface structures using fixed HeLa and living U2-OS osteosarcoma cells, respectively. Nuclei are highlighted in blue, the tubulin network is shown in green, and the actin network in red. Actin microfilaments reassemble at the cell cortex, a thin layer of filament network located close to the cell membrane. In contrast, microtubules are located in deeper portions of the cell's cytoplasm. The optical navigation provides direct selection of best locations for force volume images and single force measurements. Force measurements were conducted closer to the cell periphery rather than close to the nuclei where the indentation part of the force curve would be non-linear and thus would not fit for calculation. With this procedure the total data acquisition time decreased significantly, and the sensitive samples and probes were better preserved.

In addition, the software provides the ability to zoom, adjust color and contrast, and modify the opacity of AFM channels in the regions of interest. This facilitates good matches with optical images and supports observation of experimental pre-test and post-test studies. Finally, the vertical laser path in the Catalyst microscope head enabled much higher stability, lower noise, and increased detection sensitivity.

To further test the "Miro canvas" optical navigation in the context of force measurements as well as the sensitivity of the system, the effects of drugs interfering with the cytoskeleton integrity and, thus, cell elasticity were analyzed. Effects of cytoskeleton destabilizing agents like latrunculin and nocodazole on cell elasticity and on plasma membrane mechanics have already been investigated in various cell models [11, 15–18].

In this study, living HeLa and U2-OS osteosarcoma cells were treated with the cytoskeleton-destabilizing drugs nocodazole and latrunculin, both of which cause disruption of cytoskeletal filaments inside living cells. Latrunculin binds only to actin monomers thereby preventing its polymerization and disrupting the actin cytoskeleton. In contrast, nocodazole targets tubulin, forming a nocodazole-tubulin complex that prevents microtubule assembly and leads to the disruption of the microtubule network.

Fluorescence microscopy of treated cells showed very similar results for both nocodazole and lactrunculin on cytoskeleton integrity (Figure 2). After 30 minutes of drug exposure, cells exhibit neither red (actin) nor green (tubulin) fluorescence, indicating complete disruption of actin and tubulin networks (data not shown here). No quantifiable difference could be detected between the two cytoskeleton modulators. In contrast, AFM measurements revealed significant differences in the indentation curves recorded on cells treated with nocodazole compared to cells treated with latrunculin. A minimum of 30 force volume images were collected on each type of sample. The average Young's moduli were found to be 89.1 ± 11.4 kPa and 105.1 ± 17.2 kPa for

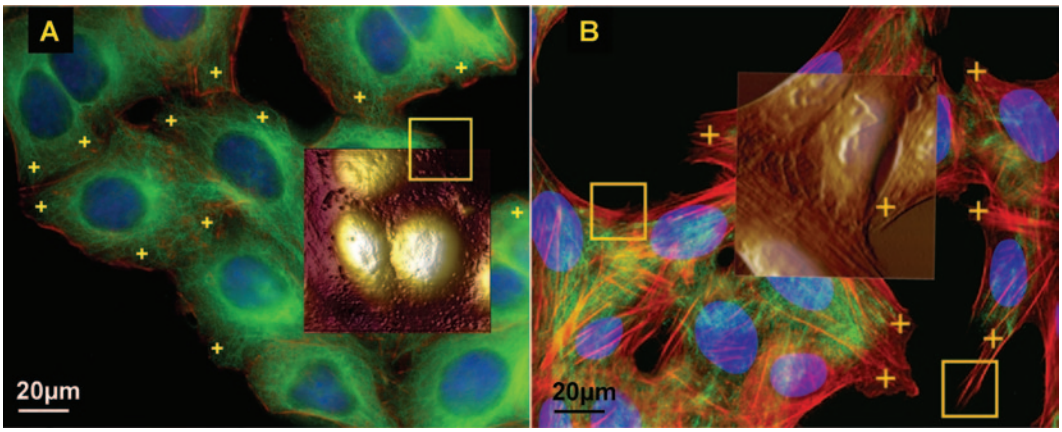

Figure 1: Overlay of AFM images with optical images (20× magnification) of fixed HeLa (A) and living U2-OS osteosarcoma cells (B). Contact and tapping mode were systematically used to check the tracking conditions. Insets show contact mode height images (75 × 75 × 5 µm) matching with the optical part of the image. A: Navigation using MIRO software was optimized on fixed HeLa cells. Nuclei are labeled with DAPI (blue), microtubules with anti-β-tubulin antibody detected by a TRITC-labeled secondary antibody (green), and actin microfilaments with Phalloidin-Alexa488 (red). B: Application of MIRO to generate force curves on preselected subcellular areas of living U2-OS-FP635-Actin cells transiently transfected with pEYFP-Tubulin. Nuclei are labeled with DAPI (blue), FP635-Actin fusion protein is indicated in red, and EYFP-Tubulin fusion protein in green. Force mode was used to probe cell elasticity in real-time. Yellow squares and crosses indicate typical locations where force-volume scans and single-force measurements were performed, respectively.

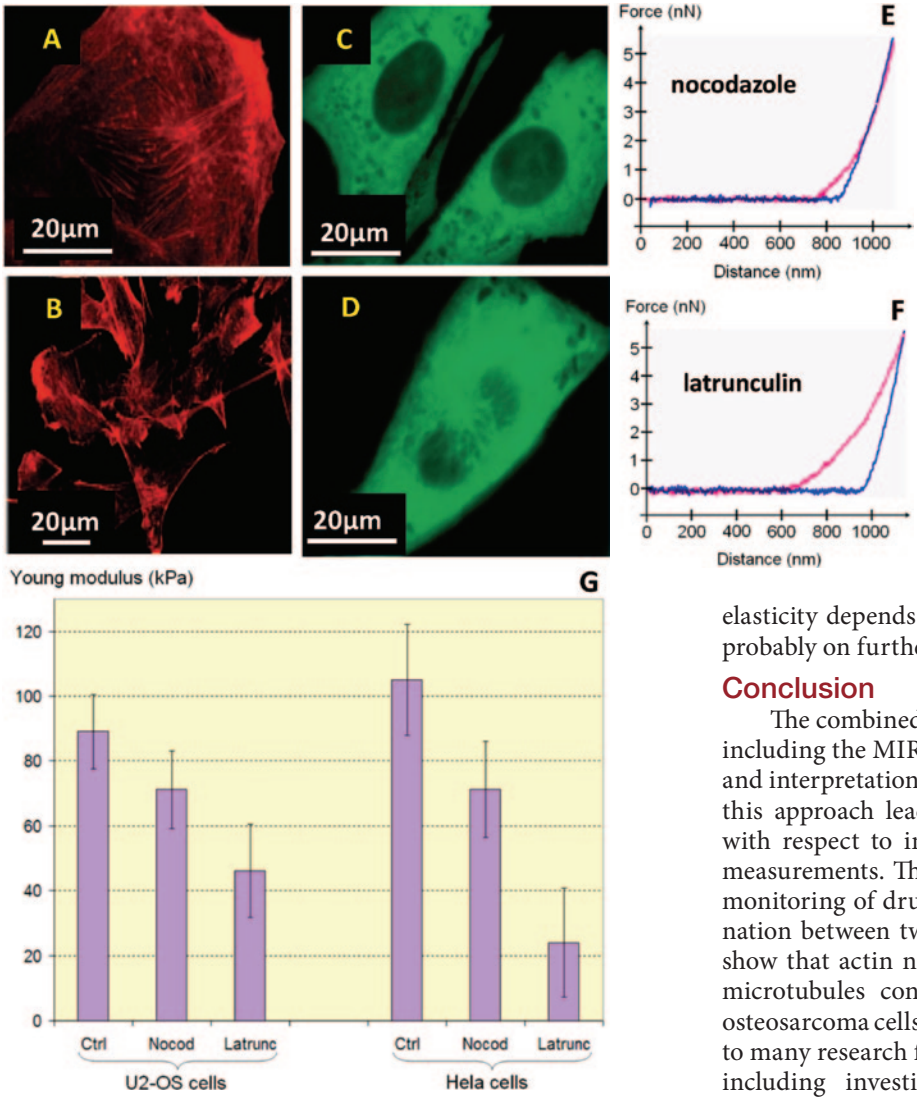

Figure 2: Effect of cytoskeleton-destabilizing drugs on cell elasticity investigated on living U2-OS and living HeLa cells. **2A–2D:** U2-OS-FP635-Actin cells (2A), U2-OS-Tag-RFP-Tubulin (2B), living HeLa cells transiently transfected with EYFP-Actin (2C) and transfected with EYFP-Tubulin (2D) were treated with nocodazole and latrunculin. Drug administration was done at a concentration of 50 µM for each drug for 30 minutes at room temperature. **2E–2F:** Representative force curves recorded on living HeLa cells exposed to nocodazole and latrunculin, respectively. Control curves are displayed in blue; curves upon drug testing are shown in purple. After calibration of the deflection sensitivity and calculation of the spring constant of each AFM cantilevers, Young's moduli were extracted by using DMT calculation. **2G:** Apparent Young's moduli for U2-OS and HeLa cells.

U2-OS and living HeLa control cells, respectively (Figure 2G). Treatment of U2-OS cells with nocodazole caused a decrease in cell stiffness of 20 percent; whereas, latrunculin treatment revealed a decrease of 48 percent. The drug-induced decrease of cell stiffness showed even stronger effects in living HeLa cells in which reductions in cell stiffness of 32 percent and 77 percent were recorded upon treatment with nocodazole and latrunculin, respectively.

These results show that AFM measurements are able to quantifiably distinguish between actin and microtubule disassembly. Force measurements have detected a greater decrease in membrane stiffness after incubation with latrunculin as with nocodazole. These data point to a significant regulation of cell stiffness by actin organization, whereas microtubules probably contribute to a lesser extent to the cytoskeleton elasticity in both the cell types. Nevertheless, microtubules have major roles in signaling pathways and important functions in the mechanical properties of the cell [17, 18]. Furthermore, force measurements allowed the identification of significant differences in cell mechanical properties between both the cancer cell lines HeLa and U2-OS. Living HeLa cells analyzed in this study may have a lesser-developed cytoskeleton compared to U2-O2 cells; this is possibly caused by an increased mitotic rate leading to a distinct decrease in cell rigidity. Obviously, the exact value and nature of such changes in cell elasticity depends on type of the cell, type of the cancer, and probably on further yet unknown promoting factors.

Conclusion

The combined setup of AFM and fluorescence microscopy including the MIRO software supports a better understanding and interpretation of AFM images of living cells. In particular, this approach leads to a more efficient application of AFM with respect to improved navigation for imaging and force measurements. This allowed an efficient *in situ* and real-time monitoring of drug effects on cell elasticity and the discrimination between two different types of cancer cells. We could show that actin network and, to a significantly lesser extent, microtubules contribute to elasticity of HeLa and U2-OS osteosarcoma cells, respectively. This approach can be extended to many research fields involving cell elasticity measurements, including investigation of cardiovascular and infectious diseases, cancer research, and drug targeting.

References

[1] S Kumar and VM Weaver, *Cancer Metastasis Rev* 28 (2009) 113–27.
[2] YK Park et al., PNAS USA 105(37) (2008) 13730–35.
[3] S Suresh, *Acta Biomaterialia* 3 (2007) 413–38.
[4] JP Mills et al., *PNAS USA* 104(22) (2007) 9213–17.
[5] HJ He et al., *BMC Cell Biol* 10 (2009) 81.
[6] SE Cross et al., *Nat Nanotechnol* 2 (2007) 780–83.
[7] I Sokolov, *Cancer Nanotechnology*, eds. HS Nalwa and T Webster, (2006) 1–17.
[8] GYH Lee and CT Lim, *Trends Biotechnol* 25(3) (2007) 111–18.
[9] KJ Van Vliet et al., *Acta Mater* 51(19) (2003) 5881–5905.
[10] HW Wu et al., *Scanning* 20 (1998) 389–97.
[11] C Rotsch and M Radmacher, *Biophys J* 78 (2000) 520–35.
[12] TK Berdyyeva et al., *Phys Med Biol* 50 (2005) 81–92.
[13] I Sokolov et al., *Nanomedicine* 2 (2006) 31–36.
[14] I Dulinska et al., *J Biochem Biophys Methods* 66 (2006) 1–3.
[15] D Weihs et al., *Phys Fluids* (2007); 19(10): 103102.
[16] C Roduit et al., *Biophys J* 94(4) (2008) 1521–32.
[17] S Kasas et al., *Cell Motil Cytoskel* 62 (2005) 124–132.
[18] AE Pelling et al., *Nanomedicine* 3 (2007) 43.

MT